Inorganic Chemistry

Article

pubs.acs.org/IC

$BiSr_3(YO)_3(BO_3)_4$: A New Gaudefroyite-Type Rare-Earth Borate with Moderate SHG Response

Jianhua Gao* and Shuai Li

National Key Laboratory of Photoelectric Technology and Functional Materials (Culture Base), Department of Physics, Northwest University, Xi'an, 710069, China

Supporting Information

ABSTRACT: The synthesis, crystal structure, crystal growth, and characterization of a new noncentrosymmetric rare-earth borate $BiSr_3(YO)_3(BO_3)_4$ are reported. $BiSr_3(YO)_3(BO_3)_4$ belongs to gaudefroyite type of structure and crystallizes in the polar hexagonal space group $P6_3$ (no. 173) with a = 10.6975(16) Å and c = 6.7222(12) Å. In the structure, the YO_7 polyhedra share edges to form an one-dimensional chain along the [001] direction. These chains are interconnected by the BO_3 group to construct a three-dimensional framework, leaving two kinds of channels for Bi atoms and Sr atoms together with BO_3 groups, respectively. On the basis of the powder second-harmonic generation (SHG) measurement, $BiSr_3(YO)_3(BO_3)_4$ belongs to the phase-matchable class with a SHG response of about 3 × KDP.

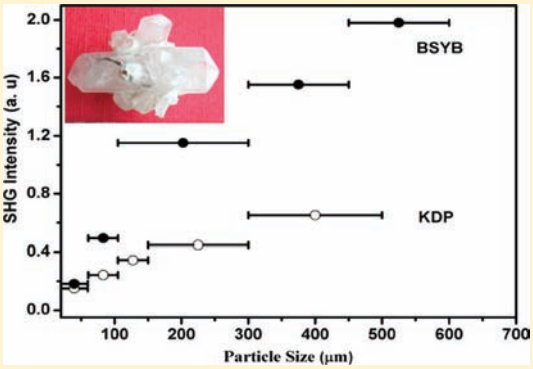

INTRODUCTION

A great deal of interest has focused on the exploration of self-frequency-doubled (SFD) laser crystals for the development of compact all-solid-state visible sources. SFD lasers have been demonstrated in a variety of Nd^{3+}- or Yb^{3+}-doped nonlinear crystal hosts, most notably $YAl_3(BO_3)_4$ (YAB),[1,2] $LiNbO_3$,[3] and $RECa_4O(BO_3)_3$ (RE = Y or Gd).[4] However, each of them has its restrictions, such as the relatively poor-quality crystal for YAB,[5] low doping concentration of lanthanide ions for $LiNbO_3$, and relatively low second-harmonic generation (SHG) efficiency for $RECa_4O(BO_3)_3$.[6] Therefore, it is very necessary to search for novel nonlinear materials containing rare-earth elements with large nonlinear optical (NLO) effects and good crystal growth habits. For this purpose, we have put the emphases on the rare-earth borates containing Bi elements. Design strategies are as follows. First, borates are often easy to grow and have the broad transparent region, high damage threshold, and moderate birefringence, for example, LiB_3O_5 (LBO)[7] and β-BaB_2O_4 (BBO).[8] Second, the combination of borates and the lone pair of the Bi^{3+} can afford large NLO effects, such as α-BiB_3O_6 (BIBO) with d_{eff} = 3.2 pm/V,[9−12] which is higher than that for most other materials currently used, like LBO and BBO. Finally, containing rare-earth elements is favorable for the substitution of other lanthanide ions, due to similar ion radii of rare-earth elements. On the basis of the abovementioned viewpoints, we investigated the quaternary systems $AO-Bi_2O_3-Y_2O_3-B_2O_3$ (A = alkaline earth metals) and found a new noncentrosymmetric compound $BiSr_3(YO)_3(BO_3)_4$ (BSYB). Herein, we report its synthesis, structure, crystal growth, NLO effect, and thermal properties. In addition, a series of isostructural compounds $BiSr_3(REO)_3(BO_3)_4$ (RE = Dy, Ho, Er, Tm, Yb, and Lu) were also synthesized.

EXPERIMENTAL SECTION

Synthesis. Polycrystalline samples of BSYB were synthesized by solid-state reaction in a Φ20 × 20 mm^3 platinum crucible with analytically pure staring materials of Bi_2O_3, $SrCO_3$, Y_2O_3, and H_3BO_3. A stoichiometric amount of reagents was mixed homogeneously and heated at 300 °C for 5 h, 500 °C for another 5 h, then ground carefully, and finally fired at 950 °C for 2 days with several intermediate grindings. The same synthesized condition was performed in the preparation process of $BiSr_3(REO)_3(BO_3)_4$ (RE = lanthanide element except for the *Pm*).

Single-Crystal Synthesis. The single crystals were grown from the SrF_2-BiBO_3 flux system. A mixture of the powder BSYB and the flux were melted homogeneously at 920 °C in a Φ20 × 20 mm^3 platinum crucible, then slowly cooled down to 750 °C at a rate of 3 °C/h, and followed by cooling to room temperature with the power off. Colorless crystals were physically separated from the matrix for structure determination.

Large Single-Crystal Growth. To obtain crystals for property measurements, crystal growth was carried out in a vertical Molysili furnace controlled by a programmable temperature controller. A mixture of the powder BSYB and the flux was melted in a Φ60 × 60 mm^3 platinum crucible at 920 °C in a muffle furnace, and then, the crucible was placed in the crystal growth furnace. The furnace was held at 920 °C for 12 h to melt homogeneously. A little ring twisted by a Φ 0.5 mm platinum wire was attached to an alumina rod, which was introduced into the furnace and made the ring plane touch with the surface of the solution. The furnace was slowly cooled at a rate of 2 °C/h. After some crystals appeared on the platinum ring, the ring with crystals was slowly drawn out of the melt. Subsequently, the

Received: August 25, 2011
Published: December 14, 2011

   dx.doi.org/10.1021/ic201858x | *Inorg. Chem.* 2012, 51, 420−424

temperature of the furnace was reraised to 920 °C to melt the other crystals on the surface of solution. After it was kept at 920 °C for 5 h, the temperature was slowly cooled to the saturation temperature. The ring with crystals was dipped into the solution, and then, the furnace was slowly cooled at a rate of 0.2 °C/h. The large crystal can be obtained according to the above methods.

Crystal Structure Determination. A colorless prism single crystal with dimensions of 0.20 mm × 0.12 mm × 0.11 mm was selected and mounted on a glass fiber. Diffraction data were collected at room temperature [296(2) K] on a Brucker Smart APEX CCD diffractometer using a monochromatic Mo Kα radiation (λ = 0.71073 Å). Intensities were corrected for Lorenz and polarization effects. The absorption correction was performed with the SADBAS program.[13] The crystal structure was solved by a direct method and refined in the SHELX-97 system.[14] All of the atoms were refined with anisotropic thermal parameters and converged for $I > 2\sigma(I)$. During the course of the refinement, Sr, Y, B, and O atoms were well resolved, but fractional occupancy of 0.93 was refined for Bi^{3+}. To retain charge balance, the Bi^{3+} and Y^{3+} ions were considered to disorder on the same site due to their same valence and similar ions radii. Attempts to refine Bi^{3+} and Sr^{2+} at one atomic site were unsuccessful. The refined proportion of Bi^{3+} and Y^{3+} ions is 0.908(2):0.092(2). The final result was tested using PLATON,[15] and no additional symmetry was found. Relevant crystallographic data were listed in Table 1. Final atomic coordinates and equivalent isotropic displacement parameters are listed in Table 2. Further details of the crystal structure investigation may be obtained from the CIF file in the Supporting Information.

Table 1. Crystal Data and Structure Refinement for $BiSr_3(YO)_3(BO_3)_4$

empirical formula	$BiSr_3Y_3B_4O_{15}$
formula weight	1021.81
temperature	296(2) K
wavelength	0.71073 Å
diffractometer	Brucker Smart APEX CCD
crystal system, space group	hexagonal, $P6_3$ (no. 173)
unit cell dimensions	a = 10.6975(16) Å
	c = 6.7222(12) Å
	V = 666.20(18) Å^3
Z, calculated density	2, 5.094 g/cm^3
absorption coefficient	38.071 mm^{-1}
F(000)	908
crystal size	0.20 mm × 0.12 mm × 0.11 mm
θ range for data collection	2.20−28.31°
limiting indices	$-12 \le h \le 14$, $-14 \le k \le 14$, $-8 \le l \le 8$
reflections collected/ unique	3989/1040 [$R_{(int)}$ = 0.0692]
completeness to θ = 27.85	98.2%
max. and min. transmission	0.7457 and 0.3451
refinement method	full-matrix least-squares on F^2
goodness-of-fit on F^2	1.062
final R indices [$I > 2\sigma(I)$]	R = 0.0334, wR = 0.0699
R indices (all data)	R = 0.0368, wR = 0.0711
Flack parameter	0.00(2)
largest diff. peak and hole	3.628 and − 2.078 e/Å^3

SHG. The SHG signals were measured using the Kurtz and Perry method.[16] Because SHG effects are known to depend strongly on particle size, crystals were ground and sieved into the following particle size ranges: <61, 61−105, 105−300, 300−450, and 450−600 μm. To make relevant comparisons with known SHG materials, the KH_2PO_4 (KDP) crystal was also ground and sieved into the similar particle size ranges. They were irradiated with a pulsed infrared beam from a Q-switched Nd:YAG laser of wavelength 1064 nm. A filter was used to absorb the fundamental and pass the 532 nm light onto a photomultiplier. A combination of a half-wave achromatic retarder and a polarizer was used to control the intensity of the incident power, which was measured with an identical photomultiplier connected to the same high-voltage source. This procedure was then repeated using the standard NLO material KDP, and the ratio of the second harmonic intensity outputs was calculated.

Table 2. Atomic Coordinates and Equivalent Isotropic Temperature Factors for $BiSr_3(YO)_3(BO_3)_4$ at Room Temperature[a]

atom	x	y	z	Ueq
M	1/3	2/3	0.11409(11)	0.003(1)
Sr	0.28229(10)	0.14454(10)	0.42667(14)	0.007(1)
Y	0.51958(9)	0.46121(9)	0.14545(14)	0.004(1)
B1	0	0	0.106(4)	0.007(4)
B2	0.1979(12)	0.4063(12	0.403(2)	0.007(2)
O1	0.7596(7)	0.5413(8)	0.0983(15)	0.015(2)
O2	0.6047(7)	0.6746(7)	0.3495(12)	0.009(2)
O3	0.1480(7)	0.0719(8)	0.0984(19)	0.019(2)
O4	0.2867(7)	0.3866(7)	0.2779(12)	0.014(2)
O5	0.4655(8)	0.6110(8)	−0.0413(12)	0.011(2)

[a]Note: M has the compositions $Bi_{0.908(2)}Y_{0.092(2)}$; Ueq is defined as one-third of the trace of the rthogonalized U_{ij} tensor.

Powder X-ray Diffraction. Powder X-ray diffraction was used to confirm the phase purity of samples. The X-ray powder diffraction data were collected on a Bruke D8 Advance diffractometer equipped with a diffracted beam monochromator set for Cu Kα radiation (λ = 1.5406 Å).

Thermoanalytical Investigations. The thermal stability was examined under static air with a differential scanning calorimeter (DSC) made by Netzsch Company (NETZSCH DSC 200PC). The samples made on ground crystals and reference (Al_2O_3) were enclosed in Pt crucibles, heated, and then cooled at a rate of 20 °C /min.

Element Analysis. The selected single crystals were weighed and dissolved in nitric acid. The element analysis of cations was performed with inductive coupling plasma (ICP) in a Leeman Profile ICP spectrometer. Anal. calcd (wt %) for $BiSr_3(YO)_3(BO_3)_4$: Bi, 20.45; Sr, 25.73; Y, 26.10; B, 4.23. Found: Bi, 20.02; Sr, 25.87; Y, 26.70; B, 4.56.

RESULTS AND DISCUSSION

Structure. In $BiSr_3(YO)_3(BO_3)_4$, there are 10 crystallographically independent atoms in the asymmetric unit. Among them, the Bi and B1 atoms locate on the special sites, and the rest of atoms occupy the general sites (Table 2). The Y atom is linked to seven O atoms to form a pentagonal bipyramid. These YO_7 polyhedra share edges to from a one-dimensional (1D) chain along the c direction (Figure 1a). The chains are bridged by $B2O_3$ groups through sharing vertex oxygen atoms to construct a three-dimensional (3D) framework, which affords two kinds of channels along the [001] direction. The smaller channel is occupied mainly by Bi ions with 90.8% occupation and only 9.2% Y content. The larger channel hosts Sr ions and isolated $B1O_3$ groups simultaneously. The $B1O_3$ groups go through the centers of the channels and are surrounded by Sr ions (Figure 1b). The Y−O bond distances range from 2.276(8) to 2.430(8) Å with the average bond length of 2.353 Å, which is in agreement with the sum of ionic radii given by Shannon: Y^{3+} (1.10 Å in coordination VII) and O^{2-} (1.24 Å in coordination IV).[17] The angle between triangular face of $B2O_3$ group and the c-axis is 21.45°, and the $B1O_3$ triangle is perpendicular to c-axis. The mean B−O bond lengths are 1.372 and 1.379 Å for $B1O_3$ and $B2O_3$ groups, respectively. The bond valence sum (BVS)[18] calculations gave values of 2.99 for B1 atoms and 2.95 for B2 atoms, which are consistent with the expected valence. The O−B−O angle is of 3 × 119.85(17)° for

dx.doi.org/10.1021/ic201858x | Inorg. Chem. 2012, 51, 420−424

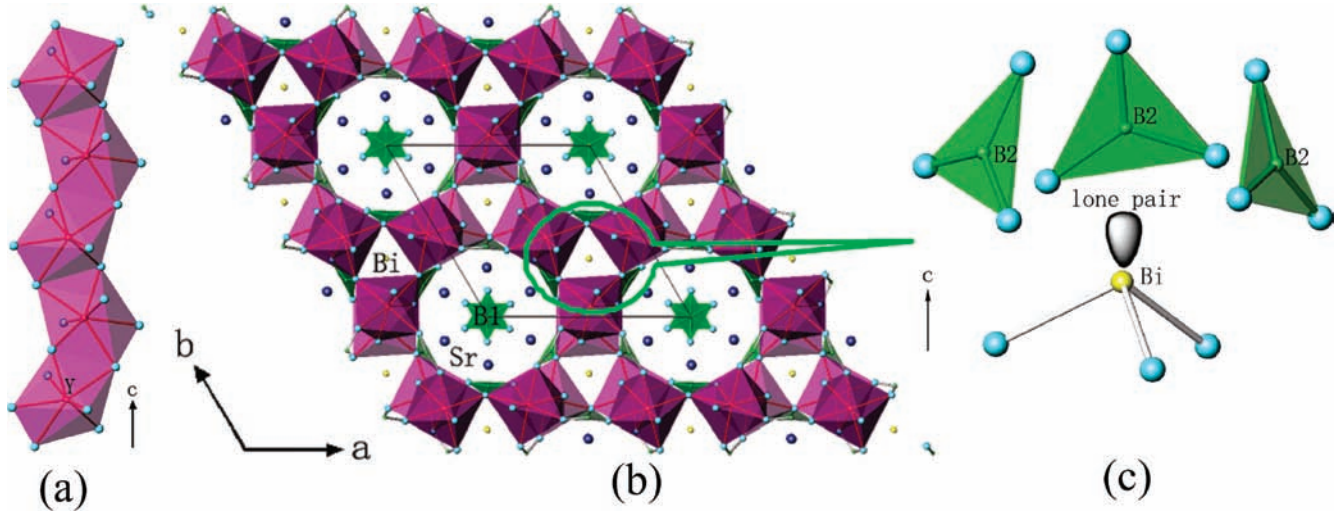

Figure 1. (a) The 1D Y−O chain, (b) the structure of $BiSr_3(YO)_3(BO_3)_4$ along the [001] direction, and (c) alignment of the $B2O_3$ triangles and BiO_3 group. Yellow balls are Bi atoms, blue balls are Sr atoms, red balls are Y atoms, green balls are B atoms, and light blue balls are O atoms. YO_7 polyhedra are purple, and BO_3 triangles are green. The gray ellipsoid represents the lone pair of Bi ions.

B1, indicating the planar triangular coordination for $B1O_3$ group, while the O−B−O angles of $B2O_3$ triangles are slightly distorted and vary from 112.9(9) to 125.0(11) °. The Bi atom coordinates to three oxygen atoms to form a pyramidal group with the Bi−O bond distance of 2.071(7) Å. BVS calculations at this site give valences of 3.19 for Bi^{3+} and 2.61 for Y^{3+}, showing that this site has valence abundance for Bi^{3+} and valence deficiency for Y^{3+}. This indicates that Bi^{3+} and Y^{3+} have a strong tendency to share a common site, which is consistent with our refinement. The situation that Bi^{3+} and Y^{3+} being disordered is also found in $(Bi_{0.6}Y_{1.4})Sn_2O_7$,[19] $Bi_{1.2}Y_{0.8}O_3$,[20] and $Bi_{7.5}Y_{0.5}O_{12}$.[21] The Sr atom is connected with eight O atoms to construct a polyhedron. The mean Sr−O bond distance is 2.644 Å [varying from 2.506(8) to 2.755(7) Å]. A BVS of 2.00 can be computed for the Sr atom, supporting that there is no disordered choice at this site (Table S1 in the Supporting Information).

The structure of title compound is isotypic with that of the mineral gaudefroyite, $Ca_4(MnO)_3(BO_3)_3CO_3$.[22−25] So far, five compounds except for the title compound have been found to belong to gaudefroyite-tpye structure. They are $YCa_3(MnO)_3(BO_3)_4$,[26] $YCa_3(AlO)_3(BO_3)_4$,[27] $YCa_3(GaO)_3(BO_3)_4$,[27] $YCa_3(VO)_3(BO_3)_4$,[28] and $BiCd_3(AlO)_3(BO_3)_4$,[29] which including $Ca_4(MnO)_3(BO_3)_3CO_3$ contain MO_6 (M = Mn, Al, Ga, and V) octahedral chains. However, in the $BiSr_3(YO)_3(BO_3)_4$, as mentioned above, the chains are formed by the distorted YO_7 polyhedra. This is the key factor to make $BiSr_3(YO)_3(BO_3)_4$ different from the other gaudefroyite compounds. These chains formed either by MO_6 or by YO_7 are bridged by BO_3 groups to from a kagomé lattice, with the trigonal and apatitelike channels. In $BiSr_3(YO)_3(BO_3)_4$, the $B2O_3$ groups play the bridge roles. Because of the distortion of Y−O chains, the $B2O_3$ groups arrange in the nearly the same direction. Also, the trigonal channel formed by YO_7 polyhedra has a smaller size and more concentrative negative charge than that by MO_6 octahedra because of the bigger volume of YO_7 polyhedron. Thus, the trigonal channels in $BiSr_3(YO)_3(BO_3)_4$ are just suitable for Bi^{3+}/Y^{3+} due to their smaller size and bigger valence, while Sr ions cannot sit in. Unlike other gaudefroyite compounds, the trigonal channels are statistically occupied by Y^{3+} and Ca^{2+}, Bi^{3+} and Cd^{2+}. In addition, the distorted Y−O chains unlike the regular MO_6 octahedral chains make the trigonal channels inhomogeneous in wideness, namely, for the space in trigonal channel, some regions are wide and some are narrow, therefore leading to the pyramidal coordination environment of Bi^{3+}. The asymmetric coordination environment of Bi^{3+} suggests the lone pair is stereoactive.[30]

In $BiSr_3(YO)_3(BO_3)_4$, the most important characteristic is the arrangement of $B2O_3$ triangles and BiO_3 groups. As shown in Figures 1c and 2, the $B1O_3$ triangles align in the opposite

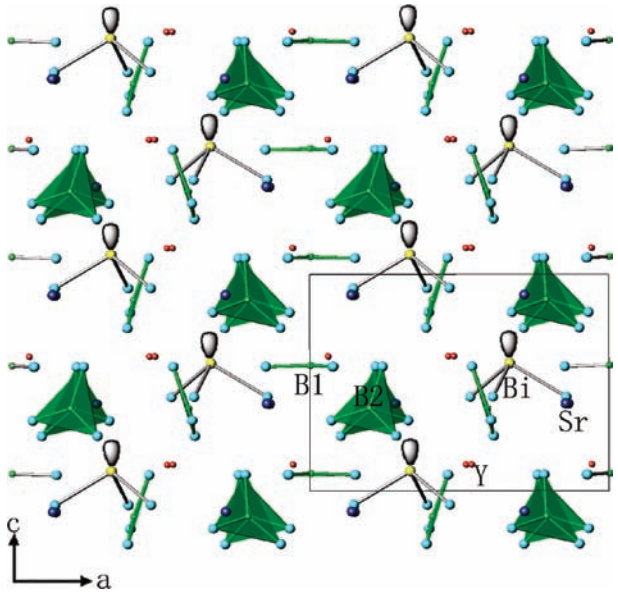

Figure 2. Structure of $BiSr_3(YO)_3(BO_3)_4$ along the *b*-axis direction. Yellow balls are Bi atoms, blue balls are Sr atoms, red balls are Y atoms, green balls are B atoms, and light blue balls are O atoms. BO_3 triangles are green. The gray ellipsoids represent lone pairs of Bi ions.

orientation, but the $B2O_3$ triangles align in the approximately same orientation, which will produce a bigger SHG effect according to the anionic group theory of NLO activity in borates.[31,32] However, in other gaudefroyite compounds, the

dx.doi.org/10.1021/ic201858x | *Inorg. Chem.* 2012, 51, 420−424

BO_3 triangles have opposite signs, and the NLO activity is canceled. The trigonal channel in $BiSr_3(YO)_3(BO_3)_4$ aforementioned accommodate Bi ions to build a Bi−O tetrahedron with stereoactive lone pair of the Bi^{3+}. More importantly, the lone pairs of all Bi^{3+} ions arrange along the *c* direction, which will also give big contributions to the SHG coefficients. The reason can deduce from the fact that the bigger SHG effect originates mainly in the same orientation alignment of the stereoactive lone pair in BiBO[9,10] (Figure S1 in the Supporting Information shows the structure of BIBO). It is worthy of noting that $BiCd_3(AlO)_3(BO_3)_4$ also crystallizes in the polar hexagonal space group $P6_3$, but the SHG contributions from BO_3 groups are canceled out due to their opposite arrangements, and the 8- or 9-coordination environment of Bi^{3+} limits the stereoactivity of lone pair; thus, the observed SHG intensity is only about 0.5 times that of KDP.[29]

NLO Property. From the above analysis, the title compound should have a bigger SHG effect due to the cooperative contributions of BO_3 groups and lone pair of the Bi^{3+}. To confirm this, the SHG effect was measured using the Kurtz and Perry method. Figure 3 shows the curve of SHG

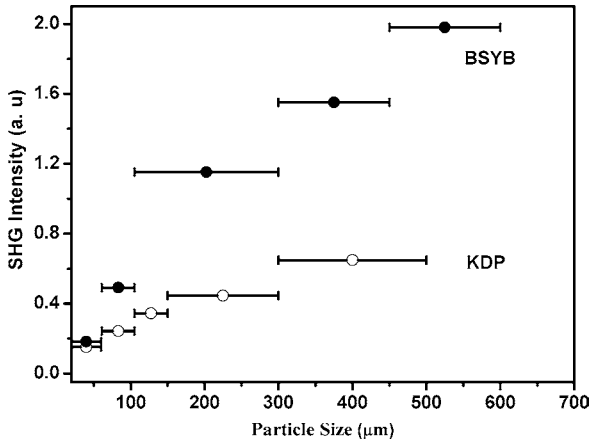

Figure 3. SHG measurements on the ground $BiSr_3(YO)_3(BO_3)_4$ (BSYB) crystals (●) with KDP (○) as the reference.

signal as a function of particle size for BSYB. The result is consistent with phase-matching behavior. The KDP was selected as the reference. The second-harmonic signal of BSYB was found to be about three times that of KDP. The result further supports above structure analysis. The more accurate nonlinear d_{eff} coefficients will be measured by a maker fringe technique[33−35] in future research.

Crystal Morphology. The Figure 4 shows the as-grown crystal obtained below 900 °C. The single crystal exhibits hexagonal prism morphology. The most perfect faces are (110) and (111) as marked in the figure. It is clear that the crystal has no cleavage cracks. Additionally, after the crystals were soaked in water for several days at room temperature, their weight had not changed obviously. These indicate that the crystal has good growth habits and excellent mechanical properties, which make it possible to produce good optical devices for NLO and SFD applications.

Thermal Behaviors. Figure 5 shows the DSC curve of BSYB and a strong signal peaking at 1094 °C. The sample enclosed in the platinum crucible was observed not to melt but to change its color from white to light brown after the DSC measurement. This implies that the endothermic peak

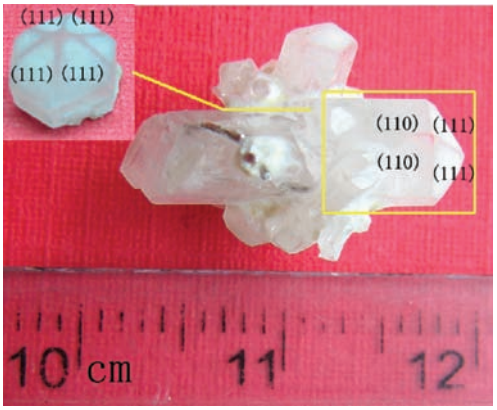

Figure 4. Photograph of the as-grown $BiSr_3(YO)_3(BO_3)_4$ crystal.

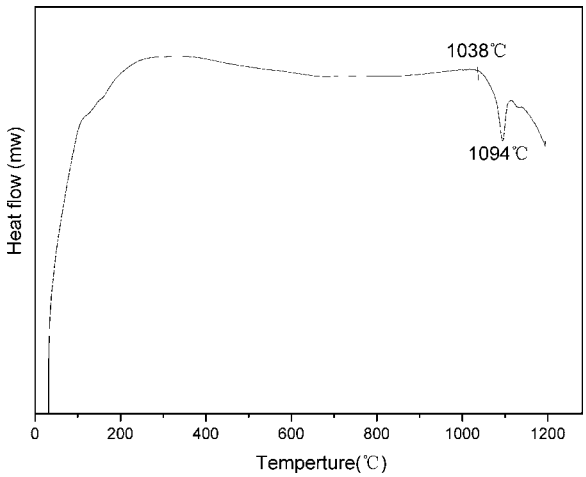

Figure 5. DSC curve of $BiSr_3(YO)_3(BO_3)_4$.

corresponds to decomposed temperature. To further verify it, some samples synthesized at 950 °C were sintered at 1100 °C. From Figure S2a,b in the Supporting Information, the powder XRD pattern of BSYB samples synthesized at 950 °C for a week is in good agreement with the theoretical one. After they were sintered at 1100 °C, the BSYB samples seem to be decomposed into $Sr_3Y_2(BO_3)_4$ and $BiYO_3$ (see Figure S2c−e in the Supporting Information). The chemical equation can be expressed as follows:

$$BiSr_3(YO)_3(BO_3)_4 \rightarrow Sr_3Y_2(BO_3)_4 + BiYO_3$$

From the above, we know that the title compound melts incongruently and its synthesized temperature cannot be higher than 1038 °C on the process of solid-state reaction.

Isostructural Compounds. A series of compounds $BiSr_3(REO)_3(BO_3)_4$ (RE = lanthanide element except for *Pm*) were also prepared at 950 °C. The derivatives of smaller rare-earth elements with a boundary between Tb and Dy can be synthesized and isostructural to the title compound. As shown in Figure S3 in the Supporting Information, XRD patterns show that $BiSr_3(REO)_3(BO_3)_4$ (RE = Dy, Ho, Er, Tm, Yb, and Lu) phases exist indeed but accompanied by some relative $Sr_3RE_2(BO_3)_4$ impurities, which may be caused by the short sintering time (only 2 days), meaning that a pure phase $BiSr_3(REO)_3(BO_3)_4$ needs a long synthesized time, maybe a week or more longer.

dx.doi.org/10.1021/ic201858x | *Inorg. Chem.* 2012, 51, 420−424

CONCLUSION

In summary, a new gaudefroyite-type rare-earth borate $BiSr_3(YO)_3(BO_3)_4$ was synthesized; it crystallizes in the polar hexagonal space group $P6_3$ with a = 10.6975(16) Å and c = 6.7222(12) Å and belongs to the gaudefroyite-type stucture. Unlike other gaudefroyite compounds, in $BiSr_3(YO)_3(BO_3)_4$, one kind of BO_3 group and BiO_3 groups with a stereoactive lone pair give big contributions to the SHG effect. The experiment using the Kurtz and Perry method also demonstrated that a SHG signal is about three times that of KDP. The large crystal of $BiSr_3(YO)_3(BO_3)_4$ is easy to grow below 900 °C, and it has good deliquescence resistance and excellent cracking resistance. In addition, a series of compounds $BiSr_3(REO)_3(BO_3)_4$ (RE = Dy, Ho, Er, Tm, Yb, and Lu) can be synthesized successfully. These advantages make it very attractive for doping high-concentration Yb, Tm, Er, and Ho ions into $BiSr_3(YO)_3(BO_3)_4$ to produce SFD crystals.

ASSOCIATED CONTENT

Supporting Information

CIF file; table for selected bond distances, angles, and BVS value; and figures for XRD patterns. This material is available free of charge via the Internet at http://pubs.acs.org.

AUTHOR INFORMATION

Corresponding Author

*E-mail: gaojh@nwu.edu.cn.

ACKNOWLEDGMENTS

Part of this work was supported by the National Natural Science Foundation of China (Grant No. 51002119) and the open funds of Key Laboratory of Functional Crystals and Laser Technology, TIPC, CAS. We thank Prof. Rukang Li and Dr. Mingjun Xia for technical help and Prof. Zhanggui Hu and Dr. Yinchao Yue for the measurement of the SHG. We also thank the anonymous reviewers for their constructive suggestions.

REFERENCES

(1) Bartschke, J.; Knappe, R.; Boller, K. J.; Wallenstein, R. *IEEE J. Quantum Electron.* **1997**, *33*, 2295.
(2) Dekker, P.; Dawes, J. M.; Piper, J. A.; Liu, Y.; Wang, J. *Opt. Commun.* **2001**, *195*, 431.
(3) Capmay, J.; Jaque, D.; Sanz Garcia, J. A.; Garcia Solé, J. *Opt. Commun.* **1999**, *161*, 253.
(4) Hammons, D. A.; Richardson, M.; Chai, B. H. T.; Chin, A. K.; Jollay, R. *IEEE J. Quantum Electron.* **2000**, *36*, 991.
(5) Jung, S. T.; Choi, D. Y.; Kang, J. K.; Chung, S. J. *J. Cryst. Growth* **1995**, *148*, 207.
(6) Aka, G.; Kahn-Harari, A.; Mougel, F.; Vivien, D.; Salin, F.; Coquelin, P.; Colin, P.; Pelenc, D.; Damelet, J. P. *J. Opt. Soc. Am. B* **1997**, *14* (9), 2238.
(7) Chen, C. T.; Wu, Y. C.; Jiang, A. D.; Wu, B. C.; You, G. M.; Li, R. K.; Lin, S. J. *J. Opt. Soc. Am. B* **1989**, *6*, 616.
(8) Chen, C. T.; Wu, B. C.; Jiang, A. D.; You, G. M. *Sci. Sin., Ser. B* **1985**, *28*, 35.
(9) Hellwig, H.; Liebertz, J.; Bohaty, L. *Solid State Commun.* **1998**, *109*, 249.
(10) Lin, Z.; Wang, Z.; Chen, C.; Lee, M. H. *J. Appl. Phys.* **2001**, *90*, 5585.
(11) Teng, B.; Wang, J.; Wang, Z.; Hu, X.; Jiang, H.; Liu, H.; Cheng, X.; Dong, S.; Liu, Y.; Shao, J. *J. Cryst. Growth* **2001**, *233*, 282.
(12) Frohlich, R.; Bohaty, L.; Liebertz, J. *Acta Crystallogr., Sect. C* **1984**, *40*, 343.
(13) Sheldrick, G. M. *SADABS*, version 2.10; Bruke Axs Inc.: Madison, WI, 1996.
(14) Sheldrick, G. M. *Acta Crystallogr., Sect. A* **2008**, *64*, 112.
(15) Spek, A. L. *J. Appl. Crystallogr.* **2003**, *36*, 7.
(16) Kurtz, S. K.; Perry, T. T. *J. Appl. Phys.* **1968**, *39*, 3798.
(17) Shannon, R. D. *Acta Crystallogr., Sect. A* **1976**, *32*, 751.
(18) Brown, I. D.; Altermatt, D. *Acta Crystallogr., Sect. B* **1985**, *41*, 244.
(19) Ismunandar.; Kennedy, B. J.; Hunter, B. A.; Vogt, T. *J. Solid State Chem.* **1997**, *131*, 317.
(20) Battle, P. D.; Catlow, C. R. A.; Heap, J. W.; Moroney, L. M. *J. Solid State Chem.* **1986**, *63*, 8.
(21) Ducke, J; Trömel, M.; Hohlwein, D.; Kizler, P. *Acta Crystallogr., Sect. C* **1996**, *52*, 1329.
(22) Jouravsky, G.; Permingeat, F. *Bull. Soc. Fr. Mineral. Cristallogr.* **1964**, *87*, 216.
(23) Yakubovich, O. V.; Simonov, M. A.; Belov, N. V. *Sov. Phys. Crystallogr.* **1975**, *20*, 87.
(24) Hoffmann, C.; Armbruster, T.; Kunz, M. *Eur. J. Mineral.* **1997**, *9*, 7.
(25) Antao, S. M.; Hassan, I. *Can. Mineral.* **2008**, *46*, 183.
(26) Li, R. K.; Greaves, C. *Phys. Rev. B* **2003**, *68*, 172403.
(27) Yu, Y.; Wu, Q. S.; Li, R. K.; J. *Solid State Chem.* **2006**, *179*, 429.
(28) Miiller, W.; Christensen, M.; Khan, A.; Sharma, N.; Macquart, R. B.; Avdeev, M.; McIntyre, G. J.; Piltz, R. O.; Ling, C. D. *Chem. Mater.* **2011**, *23*, 1315.
(29) Chen, X.; Yin, H.; Chang, X.; Zang, H.; Xiao, W. *J. Solid State Chem.* **2010**, *183*, 2910.
(30) Nguyen, S. D.; Yeon, J.; Kim, S. H.; Halasyamani, P. S. *J. Am. Chem. Soc.* **2011**, *133*, 12422.
(31) Chen, C. T.; Wu, Y. C.; Li, R. K. *Int. Rev. Phys. Chem.* **1989**, *8*, 65.
(32) Chen, C. T.; Wu, Y. C.; Li, R. K. *J. Cryst. Growth* **1990**, *99*, 790.
(33) Maker, P.; Terhune, R.; Nisenoff, M.; Savage, C. *Phys. Rev. Lett.* **1962**, *8*, 21.
(34) Jerphagnon, J.; Kurtz, S. K. *J. Appl. Phys.* **1970**, *41*, 1667.
(35) Jerphagnon, J.; Kurtz, S. K. *Phys. Rev. B* **1970**, *1*, 1739.